

Title	Preparation and characterization of biodegradable nanoparticles based on poly( $\gamma$ -glutamic acid) with L-phenylalanine as a protein carrier
Author(s)	Akagi, Takami; Kaneko, Tatsuo; Kida, Toshiyuki; Akashi, Mitsuru
Citation	Journal of Controlled Release, 108(2-3): 226-236
Issue Date	2005-11-28
Type	Journal Article
Text version	author
URL	<a href="http://hdl.handle.net/10119/4933">http://hdl.handle.net/10119/4933</a>
Rights	NOTICE: This is the author's version of a work accepted for publication by Elsevier. Takami Akagi, Tatsuo Kaneko, Toshiyuki Kida, and Mitsuru Akashi, Journal of Controlled Release, 108(2-3), 2005, 226-236, <a href="http://dx.doi.org/10.1016/j.jconrel.2005.08.003">http://dx.doi.org/10.1016/j.jconrel.2005.08.003</a>
Description	



# Preparation and characterization of biodegradable nanoparticles based on poly ( $\gamma$ -glutamic acid) with L-phenylalanine as a protein carrier

Takami Akagi<sup>a,b</sup>, Tatsuo Kaneko<sup>a,b</sup>, Toshiyuki Kida<sup>a,b</sup>, Mitsuru Akashi<sup>a,b,\*</sup>

<sup>a</sup>*Department of Molecular Chemistry, Graduate School of Engineering, Osaka University, 2-1 Yamadaoka, Suita 565-0871, Japan*

<sup>b</sup>*Core Research for Evolutional Science and Technology (CREST), Japan Science and Technology Agency (JST), Tokyo, Japan*

\* Corresponding author

Tel: +81-6-6879-7356, Fax: +81-6-6879-7359, E-mail: akashi@chem.eng.osaka-u.ac.jp (M. Akashi)

## **Abstract**

The objective of the present study was to prepare nanoparticles composed of poly ( $\gamma$ -glutamic acid) ( $\gamma$ -PGA) and L-phenylalanine ethylester (L-PAE) in order to evaluate the possibility of using these nanoparticles as protein carriers. Novel amphiphilic graft copolymers composed of  $\gamma$ -PGA as the hydrophilic backbone and L-PAE as the hydrophobic segment were successfully synthesized by grafting L-PAE to  $\gamma$ -PGA using water-soluble carbodiimide (WSC). Due to their amphiphilic properties, the  $\gamma$ -PGA-graft-L-PAE copolymers were able to form nanoparticles. The size of the  $\gamma$ -PGA nanoparticles was measured by photon correlation spectroscopy (PCS), and showed a narrow monodispersed size distribution with a mean diameter ranging from 150 to 200 nm. The solvents selected to prepare the  $\gamma$ -PGA nanoparticles by a precipitation and dialysis method affected the particle size distribution. To evaluate the feasibility of vehicles for these proteins, we prepared protein-loaded  $\gamma$ -PGA nanoparticles by surface immobilization and encapsulation methods. Ovalbumin (OVA) was used as a model protein, and was immobilized onto the  $\gamma$ -PGA nanoparticles or encapsulated into the inner core of these nanoparticles. Moreover, these OVA-encapsulated  $\gamma$ -PGA nanoparticles could be preserved by freeze-drying process. The results of cytotoxicity tests showed that the  $\gamma$ -PGA and  $\gamma$ -PGA nanoparticles did not cause any relevant cell damage. It is expected that biodegradable  $\gamma$ -PGA nanoparticles can immobilize proteins, peptides, plasmid DNA and drugs onto their surfaces and/or into the nanoparticles. These nanoparticles are potentially useful in pharmaceutical and biomedical applications.

**Keywords:** Poly ( $\gamma$ -glutamic acid); Biodegradation; Nanoparticles; Amphiphilic; Encapsulation

## 1. Introduction

Nanoparticles or colloidal particles have been widely used for targeted drug delivery and other biomedical applications [1,2]. Numerous investigators have shown that the biological distribution of drugs, proteins or DNA can be modified, both at the cellular and organ levels, using micro/nanoparticles delivery systems [3]. The nanometer size-ranges of these delivery systems offer distinct advantages for drug delivery. To achieve this objective, several micro/nano-sized biodegradable particles such as poly (lactide-*co*-glycolide) (PLGA), poly (lactic acid) (PLA) and poly ( $\epsilon$ -caprolactone) (PCL) particles have been developed [4]. The degradation rate and therefore the drug release rate can be controlled by varying the composition ratio and the molecular mass of the graft or block copolymers [5,6]. The capture of water-soluble drugs such as proteins in the nanoparticle carrier system can be carried out through various approaches. Double-emulsion solvent evaporation/extraction is a common and convenient method for the encapsulation of proteins into a polymer matrix [7]. However, the possible denaturation of the proteins at the oil-water interface limits the usage of this method. It has been reported that this interface causes conformational changes in bovine serum albumin (BSA) [8,9]. Moreover, it has a disadvantage in that the entrapment efficiency is very low. The prevention of protein denaturation and degradation, as well as a high entrapment efficiency, would be of particular importance in the preparation of nanoparticles containing water-soluble drugs such as a proteins. Therefore, this novel type of nanoparticle needs to be developed.

Recently, self-assembling block copolymers or hydrophobically modified polymers have been extensively investigated in the field of biotechnology and pharmaceuticals. Amphiphilic block or graft copolymers have been found to form self-assembled, nano-sized micelle-like aggregates of various morphologies in aqueous solution [10,11]. In general, self-assembled nanoparticles are composed of an inner hydrophobic core and an outer shell of hydrophilic groups. Hydrophobic blocks form the inner core of the structure, which act as a drug incorporation site, especially for hydrophobic drugs. Hydrophobic drugs can thus be easily entrapped within the inner core by hydrophobic interactions. These self-aggregating characteristics of amphiphilic polymers have attracted considerable attention as

effective targetable drug carriers, for example polyion complex micelles [12] and hydrophobized polysaccharides. Among the different carriers for controlled drug delivery, there has been rising interest in nano-sized self-aggregates composed of natural polysaccharides such as pullulan [13,14], curdlan [15], dextran [16], alginic acid [17] and chitosan [18]. Akiyoshi et al. reported that self-aggregated hydrogel nanoparticles could be formed from cholesterol-bearing pullulan by an intra- and/or intermolecular association in diluted aqueous solutions [19].

For the past two decades, we have studied the synthesis and clinical applications of core-corona polymeric nanoparticles composed of hydrophobic polystyrene and hydrophilic macromonomers [20]. Core-corona type polymeric nanoparticles have applications in various technological and biomedical fields, because their chemical structures can be easily controlled [21–23]. In previous studies, lectin-immobilized polystyrene nanoparticles efficiently captured human immunodeficiency virus type 1 (HIV-1) particles and gp120 antigens onto their surfaces [24,25]. These HIV-1-capturing nanoparticles were utilized as vaccine carriers, and were useful as carriers for a prophylactic vaccine against HIV-1 infection [26–28]. On the other hand, our group recently developed hydrophobically modified poly ( $\gamma$ -glutamic acid) ( $\gamma$ -PGA), prepared by the covalent attachments of L-phenylalanine ethylester (L-PAE) and L-leucine methylester (L-LM) to  $\gamma$ -PGA via an amide bond [29]. Monodispersed  $\gamma$ -PGA nanoparticles were formed by the amphiphilic properties of the  $\gamma$ -PGA-graft-L-PAE and  $\gamma$ -PGA-graft-L-LM.  $\gamma$ -PGA is a bacterially produced, water-soluble polyamide that is the object of current interest because of its natural origin and biodegradability [30–32]. This polymer is different from proteins in that peptide linkages are formed between the  $\alpha$ -amino and the  $\gamma$ -carboxylic acid groups. It is a high molecular weight polypeptide composed of  $\gamma$ -linked glutamic acid units, and its  $\alpha$ -carboxylate side chains can be chemically modified [33]. We have also developed a modified method to prepare  $\gamma$ -PGA as a drug delivery carrier [34], a tissue engineering material [35] and a thermosensitive polymer [36].

In this study, we synthesized  $\gamma$ -PGA-graft-L-PAE, and core-shell type biodegradable nanoparticles were prepared by a precipitation and dialysis method.  $\gamma$ -PGA is a hydrophilic segment which has

biodegradable components containing carboxyl functional groups at the side chains. L-PAE is a hydrophobic segment, and was chosen as a non-toxic amino acid. The aim of this study was to explore the feasibility of protein entrapment on/into  $\gamma$ -PGA nanoparticles. To evaluate their potential as a protein carrier, ovalbumin (OVA) was used as a model protein for this study. We report here the formation of these nanoparticles by characterizing their physicochemical properties, such as particle size, zeta potential and OVA loading capability to evaluate their use as a novel protein carrier. The protein release properties and cytotoxicity of these  $\gamma$ -PGA nanoparticles were also investigated.

## **2. Materials and methods**

### *2.1. Materials*

$\gamma$ -PGA (number-average molecular weight,  $M_n = 300,000$ ) was kindly donated by Meiji Seika Co, Ltd. L-phenylalanine ethylester (L-PAE) and ovalbumin (OVA) were purchased from Sigma (St. Louis MO). 1-ethyl-3-(3-dimethylaminopropyl)carbodiimide (water-soluble carbodiimide, WSC), dimethyl sulfoxide (DMSO), dimethyl formamide (DMF), dimethyl acetamide (DMAc), N-methyl-2-pyrrolidinone (NMP) and D(+)-glucose were purchased from Wako Pure Chemical Industries (Osaka, Japan).

### *2.2. Synthesis of $\gamma$ -PGA-graft-L-PAE*

$\gamma$ -PGA-graft-L-PAE copolymers were synthesized as previously described [29]. Briefly,  $\gamma$ -PGA (4.7 unit mmol) was hydrophobically modified by L-PAE (4.7 mmol) in the presence of WSC. Different amounts of WSC (4.7-9.4 mmol) per glutamic acid residue of  $\gamma$ -PGA were added (Fig. 1). The purified  $\gamma$ -PGA-graft-L-PAE was characterized by  $^1\text{H-NMR}$  and FT-IR spectroscopy. The degrees of grafting of L-PAE were controlled by altering the amount of WSC. The grafting degrees were in the range from 49 to 61 per 100 glutamic acid units of  $\gamma$ -PGA. In this experiment,  $\gamma$ -PGA-graft-L-PAE with 53 % grafting degree was used.

### 2.3. Preparation of $\gamma$ -PGA nanoparticles

Nanoparticles composed of  $\gamma$ -PGA-graft-L-PAE were prepared by a precipitation and dialysis method.  $\gamma$ -PGA-graft-L-PAE (10 mg) was dissolved in 1 ml of DMSO, DMF, DMAc and NMP, followed by addition of water at the same volume as the solvent to yield a translucent solution. The solutions were then dialyzed against distilled water using cellulose membrane tubing (50,000 molecular weight cut off) to form the nanoparticles and to remove the organic solvents for 72 hours at room temperature. The distilled water was exchanged at intervals of 12 hours. The dialyzed solutions obtained were then freeze-dried.

### 2.4. Immobilization of OVA onto $\gamma$ -PGA nanoparticles

A carboxyl group of the  $\gamma$ -PGA nanoparticles (10 mg/ml) was first activated by WSC (0-1000  $\mu$ g/ml in phosphate buffer, pH 5.8) for 20 min. The nanoparticles (5 mg) that were obtained by centrifugation (14,000  $\times$  g for 15 min) were mixed with 1 ml of OVA (2 mg/ml) in phosphate-buffered saline (PBS, pH 7.4), and the mixture was incubated at 4  $^{\circ}$ C for 24 hours. After the reaction, the centrifuged nanoparticles were washed twice with PBS or water, and resuspended at 10 mg/ml in PBS. The amount of immobilized OVA was evaluated by the Lowry method [37]. OVA-immobilized nanoparticles were added to the same volume of 4 % sodium dodecyl sulfate (SDS) to dissolve the nanoparticles, and the OVA loading content was then determined. The entrapment efficiency of OVA onto the nanoparticles was calculated as: (immobilized OVA amount onto the nanoparticles / initial feeding amount of OVA)  $\times$ 100.

### 2.5. Preparation of OVA-encapsulated $\gamma$ -PGA nanoparticles

To prepare the OVA-encapsulated  $\gamma$ -PGA nanoparticles, 0.25-4 mg of OVA was dissolved in 1 ml of PBS, and 1 ml of the  $\gamma$ -PGA-graft-L-PAE (10 mg/ml in DMSO) was added to the OVA solution. The resulting solution was centrifuged at 14,000  $\times$  g for 15 min, and repeatedly rinsed. The OVA loading content was measured by the Lowry method, as described above.

## 2.6. Photon correlation spectroscopy (PCS) and zeta potential measurements

The particle size distribution of the  $\gamma$ -PGA nanoparticles and the OVA-encapsulated nanoparticles in aqueous solutions was measured by photon correlation spectroscopy (PCS; Zetasizer 3000, Malvern Instruments, UK) with a He-Ne laser beam at a wavelength of 633 nm (scattering angle of 90°). The surface charge of the  $\gamma$ -PGA nanoparticles was determined by zeta potential measurement using a Zetasizer 3000. The nanoparticles suspension diluted with PBS (0.1 mg/ml) was used for particle size and zeta potential measurement without filtering.

## 2.7. Transmission electron microscopy (TEM) measurements

The morphologies of the  $\gamma$ -PGA nanoparticles and OVA-encapsulated nanoparticles were observed by TEM (JEOL) at 100 kV. A drop of the nanoparticle suspension was placed on a copper grid coated with collodion, and was negatively stained by 1 % ammonium molybdate.

## 2.8. *In vitro* release study to OVA-encapsulated $\gamma$ -PGA nanoparticles

The release experiment was carried out *in vitro* as follows: OVA-encapsulated  $\gamma$ -PGA nanoparticles (10mg) were suspended in 1ml of PBS, and were placed in a microtube. The concentration of OVA was 1.2 mg/ml of nanoparticle suspension. The tubes were incubated at 37 °C under moderate stirring. At different time intervals, 100  $\mu$ l samples were withdrawn, and centrifuged at 14,000  $\times$  g for 15 min. The amount of OVA released into the supernatant was determined by the Lowry method.

## 2.9. Freeze-drying

The  $\gamma$ -PGA nanoparticles (NP) and OVA-encapsulated nanoparticles (OVA loading; 90  $\mu$ g/1 mg of NP) dispersed in PBS, with or without 1, 2.5 and 5 % glucose as a cryoprotectant, were frozen in liquid nitrogen for 10 min and freeze-dried for 24 hours. The particle size of the freeze-dried nanoparticles redispersed into water (10 mg/ml) was compared with the initial particle size measured just before



freeze-drying. To evaluate the effects of freeze-drying on OVA released from the OVA-encapsulated nanoparticles, the amount of OVA released from the redispersed nanoparticles was measured.

### *2.10. Evaluation of the cytotoxicity of $\gamma$ -PGA nanoparticles*

The cell viability test was chosen as a cytotoxicity index, and was determined using the dye exclusion test with trypan blue. HL-60 cells were incubated in RPMI-1640 medium (Nikken Biomedical Laboratory, Kyoto, Japan) supplemented with 10 % heat-inactivated fetal bovine serum, 100 U/ml penicillin and 100  $\mu$ g/ml streptomycin (all from Gibco-BRL, Rockville, MD). The cells ( $1 \times 10^5$  cells) were then cultured with varying concentrations of  $\gamma$ -PGA (unmodified linear polymer) or nanoparticles in a 96-well microplate for 1, 2 and 3 days under a 5 % CO<sub>2</sub> atmosphere at 37 °C. After the incubation period, the cells were counted with the dye exclusion test, and the viability of the HL-60 cells was calculated. Different concentrations (0, 62.5, 125, 250, 500 and 1000  $\mu$ g/ml) of  $\gamma$ -PGA or nanoparticles were tested in triplicate.

## **3. Results and discussion**

### *3.1. Synthesis of $\gamma$ -PGA-graft-L-PAE*

Amphiphilic  $\gamma$ -PGA was synthesized by the conjugation of L-PAE as the hydrophobic groups (Fig. 1). The  $\gamma$ -PGA-graft-L-PAE could form nanoparticles due to its amphiphilic characteristics. Graft copolymers with different degrees of L-PAE grafting were prepared by changing the molar ratio of the glutamic acid units of  $\gamma$ -PGA to WSC [29]. WSC reacts with the carboxyl groups of  $\gamma$ -PGA to form an active ester intermediate, which reacts with a primary amine group from the L-PAE to form an amide bond. The degree of grafting of L-PAE was determined by <sup>1</sup>H-NMR using the integrals of the methylene peaks of  $\gamma$ -PGA, and the phenyl group peaks of phenylalanine. The degree of L-PAE grafting ranged from 49 to 61 per 100 glutamic acid units of  $\gamma$ -PGA. In this experiment,  $\gamma$ -PGA-graft-L-PAE with 53 L-PAE per 100 glutamic acid units of  $\gamma$ -PGA was used.

### 3.2. Characterization of $\gamma$ -PGA nanoparticles

The  $\gamma$ -PGA-graft-L-PAE is readily soluble in DMSO, DMF, DMAc, NMP and chloroform. Various water miscible solvents were used to prepare nanoparticles of  $\gamma$ -PGA-graft-L-PAE using a precipitation and dialysis method. It has been reported that the solvent selected to dissolve the amphiphilic polymer can influence the particle size, drug loading and physicochemical properties of the nanoparticles [14,38]. In this study, four water miscible solvents, DMSO, DMF, DMAc and NMP, were used. The size distribution of the  $\gamma$ -PGA nanoparticles was measured by PCS, and the results are shown in Fig. 2. Table 1 summarizes the particle size, zeta potential and entrapment efficiency of OVA into the nanoparticles for the various solvents. Although the mean diameter of the  $\gamma$ -PGA nanoparticles did not differ significantly based on the initial solvent used, NMP induced a broader size distribution than the other initial solvents. In the case of DMSO, the size distribution was relatively smaller than that of the other solvents. TEM observation of the nanoparticles prepared from DMSO and NMP are shown in Fig. 3. In the case of DMSO, the morphologies of the nanoparticles were spherical, with diameters ranged from about 100 to 200 nm. When NMP was used as the initial solvent, various sized nanoparticles were observed. This result was in accordance with the particle size from the PCS measurements. These results indicated that the solvent used significantly affected the distribution of the particle size. These differences are possibly related to the solubility of  $\gamma$ -PGA-graft-L-PAE in the solvent, and the diffusion rate of the organic solvent into the water. Therefore, in subsequent experiments, DMSO was used as the initial solvent.

The zeta potential did not differ significantly according to the initial solvent used. The  $\gamma$ -PGA nanoparticles had a strongly negative zeta potential ( $-20$  mV), which can be attributed to the presence of carboxyl groups located near the surface. The structure of the nanoparticles consists of a L-PAE core with an outer  $\gamma$ -PGA shell. The zeta potential value is an important particle characteristic, because it can influence particle stability. Electrostatic repulsion between particles with the same electric charge prevents the aggregation of these particles [39].

### 3.3. Entrapment of OVA on/into $\gamma$ -PGA nanoparticles

OVA-surface immobilized and inner encapsulated  $\gamma$ -PGA nanoparticles were prepared in order to study their potential application as protein carriers. The entrapment of OVA on/into the nanoparticles was successfully achieved. The amount of OVA immobilized onto the nanoparticle surface increased upon increasing the concentration of WSC (Fig. 4). OVA was immobilized onto the nanoparticles by an amide bond between the carboxyl group on surface of the  $\gamma$ -PGA nanoparticles and the amide group of OVA. As compared to untreated nanoparticles, the OVA-immobilized nanoparticles did not change their particle size, and showed a monomodal and narrow size distribution (data not shown).

Similarly, the amount of OVA encapsulated into the nanoparticles was increased upon increasing the initial feeding amount of OVA (Fig. 5). In the case of the encapsulation method, the OVA entrapment efficiency reached about 50 wt.% at maximum. The encapsulation efficiency was obviously increased with an increase in the initial OVA concentration. In addition, this result was confirmed by sodium dodecyl sulphate-polyacrylamide gel electrophoresis (SDS-PAGE) analysis. The OVA-encapsulated nanoparticles exhibited one band corresponding to a molecular weight of 45 kDa (data not shown). We hypothesized that this efficient OVA encapsulation was due to the hydrophobic interaction between the hydrophobic regions of OVA and the hydrophobic L-PAE groups. On the other hand, the entrapment efficiency of immobilization onto the surface of the nanoparticles using WSC was only about 5 %. These results demonstrated that the entrapment efficiency of OVA was significantly dependent on the conjugation method. The degree of grafting of L-PAE did not markedly influence the entrapment efficiency of OVA into the nanoparticles (data not shown).

From the PCS measurements, the mean diameter of the unloaded  $\gamma$ -PGA nanoparticles was  $149 \pm 35$  nm, with a narrow size distribution. The particle size of the nanoparticles was greatly increased when the OVA was encapsulated. Fig. 6 shows that the size of the  $\gamma$ -PGA nanoparticles increased depending on the amount of OVA loaded into the nanoparticles. The size of the OVA-encapsulated nanoparticles increased with increasing OVA content, likely due to an increase in swelling capacity due to the hydrophilic properties of OVA. Na et al. have reported that the introduction of vitamin H into

hydrophobically modified pullulan, pullulan acetate, enhanced the formation of swelling hydrogel nanoparticles due to the hydrophilicity of vitamin H [40]. Furthermore, the TEM observations demonstrated that the OVA-encapsulated nanoparticles were spherical in shape (Fig. 7). OVA-encapsulated nanoparticles with high OVA loading (OVA content over 150  $\mu\text{g}/1\text{ mg}$  of NP) formed aggregates.

#### 3.4. Release behavior of OVA-encapsulated $\gamma$ -PGA nanoparticles

To study the protein release behavior, OVA-encapsulated  $\gamma$ -PGA nanoparticles were simply suspended in PBS, and OVA release was determined *in vitro*. The release of OVA from nanoparticles with an OVA content of 120  $\mu\text{g}/1\text{ mg}$  of NP was carried out at 37 °C in PBS (pH 7.4). The OVA encapsulated into the nanoparticles was not released (less than 5 %), even after 10 days. The degree of grafting of L-PAE did not influence this release behavior (data not shown). This result indicated that the surface of the  $\gamma$ -PGA nanoparticle created a tight bond, and the protein was not released from the interior of the nanoparticles. In addition, the absence or slow release of OVA from the nanoparticles could be understood as a consequence of the interaction between the protein and the  $\gamma$ -PGA-graft-L-PAE. Moreover, this result suggested that the  $\gamma$ -PGA backbone composed of  $\gamma$ -linked glutamic acid and the amide bond between the  $\alpha$ -carboxylate side chains of the  $\gamma$ -PGA and L-PAE were not degraded under these experimental conditions. In fact, several studies have shown that the  $\gamma$ -PGA was not degraded in neutral buffer [41].

#### 3.5. Suitability of $\gamma$ -PGA nanoparticles for freeze-drying

Since freeze-drying is a convenient technique for nanoparticle storage, the effects of freeze-drying on the size of the  $\gamma$ -PGA nanoparticles and the OVA-encapsulated nanoparticles were studied. After freeze-drying, these nanoparticles were redispersed in water, and their particle size was compared to the corresponding untreated nanoparticles. The lyophilized  $\gamma$ -PGA nanoparticles were easily redispersed, and the size of the nanoparticles showed no change in initial particle size as compared to before

freeze-drying. On the other hand, lyophilized OVA-encapsulated (90  $\mu\text{g}/1\text{ mg}$  of NP) nanoparticles underwent irreversible aggregation (more than 1  $\mu\text{m}$ ) after redispersion in water. However, the addition of glucose as a cryoprotectant tended to decrease this aggregation (Fig. 8). Although in 1 % glucose aggregation above 1  $\mu\text{m}$  still remained, in the presence of 2.5 % glucose, no large aggregation was observed, and the size of the nanoparticles was preserved.

Fig. 9 shows the effects of freeze-drying on the OVA release from the OVA-encapsulated nanoparticles. The untreated and lyophilized OVA-encapsulated nanoparticles exhibited a similar release behavior. The total amount of OVA leaked from lyophilized nanoparticles with or without glucose was 3.1 and 6.8 %, respectively. Over a 1-week storage period, both untreated and lyophilized nanoparticles released less than 5 % of the OVA loaded. These results indicated that the  $\gamma$ -PGA nanoparticles and OVA-encapsulated nanoparticles had high stability for the freeze-drying process.

### 3.6. *In vitro* cytotoxicity test

The biocompatibility of the  $\gamma$ -PGA and unloaded  $\gamma$ -PGA nanoparticles was evaluated *in vitro* by a cytotoxicity test using HL-60 cells. The surviving cells after incubation was evaluated by the trypan blue exclusion assay. Fig. 10 shows the HL-60 cell proliferation and viability as a function of the concentration of  $\gamma$ -PGA and empty nanoparticles after 1-3 days of incubation. Cell proliferation was not affected by the  $\gamma$ -PGA and nanoparticles (Figure 10a, b), and cellular viability was maintained at levels higher than 90 % for both  $\gamma$ -PGA and nanoparticles, even at high concentrations (1 mg/ml) (Figure 10c, d). This implied that these  $\gamma$ -PGA nanoparticles could be useful as protein carriers without any significant cytotoxic effects.

## 4. Conclusion

Novel  $\gamma$ -PGA-graft-LPAE copolymers formed nanoparticles with a mean diameter around 200 nm and a narrow size distribution when prepared by a precipitation and dialysis method. Zeta potential measurements suggested that the  $\gamma$ -PGA nanoparticles had a core-shell type structure, with  $\gamma$ -PGA

chains placed preferentially on the outer surface and a L-PAE core. OVA as a model protein was successfully entrapped on/into these nanoparticles. *In vitro* cytotoxicity testing showed that the present nanoparticles did not induce any cytotoxicity against HL-60 cells. Therefore, these  $\gamma$ -PGA nanoparticles may be considered promising biodegradable and biocompatible protein carriers for modulated biodistribution, and site and/or cell-specific drug delivery systems. With further studies, these nanoparticles could be useful as vaccine carriers for systemic and mucosal administration.

### **Acknowledgment**

This work was supported by Core Research for Evolutional Science and Technology (CREST) from the Japan Science and Technology Agency (JST).

### **References**

- [1] T.M. Allen, P.R. Cullis, Drug delivery systems: Entering the mainstream, *Science* 303 (2004) 1818–1822.
- [2] K.S. Soppimath, T.M. Aminabhavi, A.R. Kulkarni, W.E. Rudzinski, Biodegradable polymeric nanoparticles as drug delivery devices, *J. Control. Release* 70 (2001) 1–20.
- [3] J. Panyam, V. Labhasetwar, Biodegradable nanoparticles for drug and gene delivery to cells and tissue, *Adv. Drug Deliv. Rev.* 55 (2003) 329–347.
- [4] M.L. Hans, A.M. Lowman, Biodegradable nanoparticles for drug delivery and targeting, *Curr. Opin. Solid State Mater. Sci.* 6 (2002) 319–327.
- [5] D.T. O'Hagan, H. Jeffery, S.S. Davis, The preparation and characterization of poly(lactide-co-glycolide) microparticles: III. Microparticle/polymer degradation rates and the *in vitro* release of a model protein, *Int. J. Pharm.* 103 (1994) 37–45.

- [6] X. Li, X. Deng, M. Yuan, C. Xiong, Z. Huang, Y. Zhang, W. Jia, In vitro degradation and release profiles of poly-DL-lactide-poly(ethylene glycol) microspheres with entrapped proteins, *J. Appl. Polym. Sci.* 78 (2000) 140–148.
- [7] P. Quellec, R. Gref, L. Perrin, E. Dellacherie, F. Sommer, J.M. Verbavatz, M.J. Alonso, Protein encapsulation within polyethylene glycol-coated nanospheres. I. Physicochemical characterization, *J. Biomed. Mater. Res.* 42 (1998) 45–54.
- [8] H. Sah, Stabilization of proteins against methylene chloride / water interface induced denaturation and aggregation, *J. Control. Release* 58 (1999) 143–151.
- [9] J. Panyam, M.M. Dali, S.K. Sahoo, W. Ma, S.S. Chakravarthi, G.L. Amidon, R.J. Levy, V. Labhasetwar, Polymer degradation and in vitro release of a model protein from poly(D,L-lactide-co-glycolide) nano- and microparticles, *J. Control. Release* 92 (2003) 173–187.
- [10] L. Zhang, A. Eisenberg, Multiple morphologies and characteristics of “crew-cut” micelle-like aggregates of polystyrene-*b*-poly(acrylic acid) diblock copolymers in aqueous solutions, *J. Am. Chem. Soc.* 118 (1996) 3168–3181.
- [11] X.M. Liu, K.P. Pramoda, Y.Y. Yang, S.Y. Chow, C. He, Cholesteryl-grafted functional amphiphilic poly(N-isopropylacrylamide-co-N-hydroxymethylacrylamide): synthesis, temperature sensitivity, self-assembly and encapsulation of a hydrophobic agent, *Biomaterials* 25 (2004) 2619–2628.
- [12] M. Jaturanpinyo, A. Harada, X. Yuan, K. Kataoka, Preparation of bionanoreactor based on core-shell structured polyion complex micelles entrapping trypsin in the core cross-linked with glutaraldehyde, *Bioconjugate Chem.* 15 (2004) 344–348.
- [13] K. Akiyoshi, S. Kobayashi, S. Shichibe, D. Mix, M. Baudys, S.W. Kim, J. Sunamoto, Self-assembled hydrogel nanoparticle of cholesterol-bearing pullulan as a carrier of protein drugs: Complexation and stabilization of insulin, *J. Control. Release* 54 (1998) 313–320.

- [14] S.W. Jung, Y.I. Jeong, S.H. Kim, Characterization of hydrophobized pullulan with various hydrophobicities, *Int. J. Pharm.* 254 (2003) 109–121.
- [15] K. Na, K.H. Park, S.W. Kim, Y.H. Bae, Self-assembled hydrogel nanoparticles from curdlan derivatives: characterization, anti-cancer drug release and interaction with a hepatoma cell line (HepG2), *J. Control. Release* 69 (2000) 225–236.
- [16] R. Gref, J. Rodrigues, P. Couvreur, Polysaccharides grafted with polyesters: novel amphiphilic copolymers for biomedical applications, *Macromolecules* 35 (2002) 9861–9867.
- [17] M. Leonard, M.R.D. Boisseson, P. Hubert, F. Dalencon, E. Dellacherie, Hydrophobically modified alginate hydrogels as protein carriers with specific controlled release properties, *J. Control. Release* 98 (2004) 395–405.
- [18] J.H. Park, S. Kwona, J.O. Nam, R.W. Park, H. Chung, S.B. Seo, I.S. Kim, I.C. Kwon, S.Y. Jeong, Self-assembled nanoparticles based on glycol chitosan bearing 5 $\alpha$ -cholanic acid for RGD peptide delivery, *J. Control. Release* 95 (2004) 579–588.
- [19] K. Akiyoshi, S. Deguchi, N. Moriguchi, S. Yamaguchi, J. Sunamoto, Self-aggregates of hydrophobized polysaccharides in water. Formation and characteristics of nanoparticles, *Macromolecules* 26 (1993) 3062–3068.
- [20] M. Akashi, T. Yanagi, E. Yashima, N. Miyauchi, Graft copolymers having hydrophobic backbone and hydrophilic branches. IV. A copolymerization study of water-soluble oligovinylpyrrolidone macromonomers, *J. Polym. Sci. Part A: Polym. Chem.* 27 (1989) 3521–3530.
- [21] S. Sakuma, N. Suzuki, H. Kikuchi, K. Hiwatari, K. Arikawa, A. Kishida, M. Akashi, Oral peptide delivery using nanoparticles composed of novel graft copolymers having hydrophobic backbone and hydrophilic branches, *Int. J. Pharm.* 149 (1997) 93–106.



- [22] C.W. Chen, T. Serizawa, M. Akashi, Preparation of platinum colloids on polystyrene nanospheres and their catalytic properties in hydrogenation, *Chem. Mater.* 11 (1999) 1381–1389.
- [23] T. Serizawa, K. Taniguchi, M. Akashi, Hetero-coagulation of polymeric core-corona microspheres, *Colloids Surf.* 169 (2000) 95–105.
- [24] M. Akashi, T. Niikawa, T. Serizawa, T. Hayakawa, M. Baba, Capture of HIV-1 gp120 and virions by lectin-immobilized polystyrene nanospheres, *Bioconjugate Chem.* 9 (1998) 50–53.
- [25] T. Hayakawa, M. Kawamura, M. Okamoto, M. Baba, T. Niikawa, S. Takehara, T. Serizawa, M. Akashi, Concanavalin A-immobilized polystyrene nanospheres capture HIV-1 virions and gp120: potential approach towards prevention of viral transmission, *J. Med. Virol.* 56 (1998) 327–331.
- [26] M. Kawamura, T. Naito, M. Ueno, T. Akagi, K. Hiraishi, I. Takai, M. Makino, T. Serizawa, K. Sugimura, M. Akashi M. Baba, Induction of mucosal IgA following intravaginal administration of inactivated HIV-1-capturing nanospheres in mice, *J. Med. Virol.* 66 (2002) 291–298.
- [27] T. Akagi, M. Kawamura, M. Ueno, K. Hiraishi, M. Adachi, T. Serizawa, M. Akashi, M. Baba, Mucosal immunization with inactivated HIV-1-capturing nanospheres induces a significant HIV-1-specific vaginal antibody response in mice, *J. Med. Virol.* 69 (2003) 163–172.
- [28] A. Miyake, T. Akagi, Y. Enose, M. Ueno, M. Kawamura, R. Horiuchi, K. Hiraishi, M. Adachi, T. Serizawa, O. Narayan, M. Akashi, M. Baba, M. Hayami, Induction of HIV-specific antibody response and protection against vaginal SHIV transmission by intranasal immunization with inactivated SHIV-capturing nanospheres in macaques, *J. Med. Virol.* 73 (2004) 368–377.
- [29] M. Matsusaki, K. Hiwatari, M. Higashi, T. Kaneko, M. Akashi, Stably-dispersed and surface-functional bionanoparticles prepared by self-assembling amphipathic polymers of hydrophilic poly( $\gamma$ -glutamic acid) bearing hydrophobic amino acids, *Chem. Lett.* 33 (2004) 398–399.

- [30] H. Kubota, T. Matsunobu, K. Uotani, H. Takebe, A. Satoh, T. Tanaka, M. Taniguchi, Production of poly( $\gamma$ -glutamic acid) by *Bacillus subtilis* F-2-01, *Biosci. Biotech. Biochem.* 57 (1993) 1212–1213.
- [31] F.B. Oppermann, S. Fickaitz, A. Steinbuchel, A, Biodegradation of polyamides, *Polym. Degrad. Stab.* 59 (1998) 337–344.
- [32] M. Obst, A. Steinbuchel, Microbial degradation of poly(amino acid)s, *Biomacromolecules* 5 (2004) 1166–1176.
- [33] E.C. King, W.J. Watkins, A.J. Blacker, T.D.H. Bugg, Covalent modification in aqueous solution of poly- $\gamma$ -D-glutamic acid from *Bacillus licheniformis*, *J. Polym. Sci. A: Polym. Chem.* 36 (1998) 1995–1999.
- [34] A. Kishida, K. Murakami, H. Goto, M. Akashi, H. Kubota, T. Endo, Polymer drugs and polymeric drugs X: Slow release of 5-fluorouracil from biodegradable poly( $\gamma$ -glutamic acid) and its benzyl ester matrixes, *J. Bioact. Compat. Polym.* 13 (1998) 270–278.
- [35] M. Matsusaki, T. Serizawa, A. Kishida, T. Endo, M. Akashi, Novel functional biodegradable polymer: synthesis and anticoagulant activity of poly( $\gamma$ -glutamic acid)sulfonate ( $\gamma$ -PGA-sulfonate), *Bioconjugate Chem.* 13 (2002) 23–28.
- [36] T. Shimokuri, T. Kaneko, T. Serizawa, M. Akashi, Preparation and thermosensitivity of naturally occurring polypeptide poly( $\gamma$ -glutamic acid) derivatives modified by propyl groups, *Macromol. Biosci.* 4 (2004) 407–411.
- [37] G.L. Peterson, A simplification of the protein assay method of Lowry et al. which is more generally applicable, *Anal. Biochem.* 83 (1977) 346–356.
- [38] J.G. Ryu, Y.I. Jeong, I.S. Kim, J.H. Lee, J.W. Nah, S.H. Kim, Clonazepam release from core-shell type nanoparticles of poly( $\epsilon$ -caprolactone):poly(ethylene glycol): poly( $\epsilon$ -caprolactone) triblock copolymers, *Int. J. Pharm.* 200 (2000) 231–242.

[39] S.S Feng, G. Huang, Effects of emulsifiers on the controlled release of paclitaxel (Taxol) from nanospheres of biodegradable polymers, *J. Control.Release* 71 (2001) 53–69.

[40] K. Na, T.B. Lee, K.H. Park, E.K. Shin, Y.B. Lee, H.K. Choi, Self-assembled nanoparticles of hydrophobically-modified polysaccharide bearing vitamin H as a targeted anti-cancer drug delivery system, *Eur. J. Pharm. Sci.* 18 (2003) 165–173.

[41] F. Kesuo, G. Denis, S. Martin, Hydrolytic and enzymic degradation of poly( $\gamma$ -glutamic acid) hydrogels and their application in slow-release systems for proteins. *J. Environ. Polym. Degrad.* 4 (1996) 253–260.

## Figure caption

Table 1 Particle size, zeta potential and OVA loading content of  $\gamma$ -PGA nanoparticles according to the initial solvent used

Fig. 1. Chemical structure of  $\gamma$ -PGA and synthesis scheme for  $\gamma$ -PGA-graft-L-PAE.

Fig. 2. Particle size distribution of  $\gamma$ -PGA nanoparticles as measured by PCS according to the initial solvent used: (●) DMSO, (○) DMF, (△) DMAc and (□) NMP. The nanoparticles were prepared by a precipitation and dialysis method.

Fig. 3. TEM images of  $\gamma$ -PGA nanoparticles prepared with (a) DMSO and (b) NMP as the initial solvent. The nanoparticles were counterstained with 1 % ammonium molybdate.

Fig. 4. Effect of the WSC concentration on the amount of OVA immobilized onto  $\gamma$ -PGA nanoparticles. The  $\gamma$ -PGA nanoparticles were treated with various amounts of WSC, and OVA was mixed to a final concentration of 2 mg/ml. The amount of OVA entrapped was calculated by the immobilized OVA weight ( $\mu\text{g}$ ) / nanoparticles weight (1 mg). The results are presented as mean  $\pm$  SD values (n = 3).

Fig. 5. Effect of the OVA concentration on the amount of OVA encapsulated (●) into the  $\gamma$ -PGA nanoparticles and the entrapment efficiency (○).  $\gamma$ -PGA-graft-L-PAE (in DMSO) and OVA were mixed to a final copolymer concentration of 5 mg/ml. The amount of OVA entrapped was calculated by the encapsulated OVA weight ( $\mu\text{g}$ ) / nanoparticle weight (1 mg). The entrapment efficiency was measured as the total encapsulated OVA weight / initial OVA weight  $\times$  100. The results are presented as means  $\pm$  SD values (n = 3).

Fig. 6. Changes in the size of the  $\gamma$ -PGA nanoparticles with increasing encapsulated OVA content. The size of the OVA-encapsulated nanoparticles was measured in PBS by PCS using a Zetasizer 3000.

Fig. 7. TEM images of OVA-encapsulated  $\gamma$ -PGA nanoparticles. The OVA-encapsulated (90  $\mu\text{g}/1\text{ mg}$  of NP) nanoparticles were counterstained with 1 % ammonium molybdate.

Fig. 8. Effect of freeze-drying in the presence of glucose as a cryoprotectant on the size of OVA-encapsulated (90  $\mu\text{g}/1\text{ mg}$  of NP)  $\gamma$ -PGA nanoparticles. The size before freeze-drying (●), after freeze-drying (○) and during freeze-drying with 2.5 % glucose (△) was measured in PBS by dynamic light scattering (DLS).

Fig. 9. Effect of freeze-drying in the presence of glucose as a cryoprotectant on the release of OVA from OVA-encapsulated (90  $\mu\text{g}/1\text{ mg}$  of NP)  $\gamma$ -PGA nanoparticles.

Fig. 10. Evaluation of the cytotoxicity against HL-60 cells of  $\gamma$ -PGA (a, c) and  $\gamma$ -PGA nanoparticles (b, d) at various concentrations: (●) untreated, (○) 62.5, (△) 125, (□) 250, (◇) 500 and (\*) 1000  $\mu\text{g}/\text{ml}$ . Cell proliferation (left) was determined by cell counting after 1, 2 and 3 days of incubation. The cell viability (right) expressed in % was calculated as  $[(N_s - N_d) / (N_s + N_d)] \times 100$ , where  $N_s$  and  $N_d$  are the number of surviving cells and dead cells, respectively.

# Table 1

Table 1

Particle size, zeta potential and OVA loading content of  $\gamma$ -PGA nanoparticles according to the various initial solvent used

Solvent	Mean diameter $\pm$ SD (nm) <sup>a</sup>	C.V. (%) <sup>b</sup>	Zeta potential (mV) <sup>c</sup>	Entrapment efficiency (wt. %) <sup>d</sup>
DMSO	149 $\pm$ 35	23.6	-23.1	46.6
DMF	152 $\pm$ 44	28.9	-23.9	43.5
DMAc	159 $\pm$ 50	31.6	-22.9	47.1
NMP	194 $\pm$ 115	59.3	-23.3	45.1

<sup>a</sup> Particle size distribution of  $\gamma$ -PGA nanoparticles was measured in PBS by photon correlation spectroscopy (PCS).

<sup>b</sup> C.V. (coefficient of variation) = S.D. (standard deviation) / mean diameter.

<sup>c</sup> Zeta potential of  $\gamma$ -PGA nanoparticles was measured in PBS by a Zetasizer 3000.

<sup>d</sup>  $\gamma$ -PGA-graft-L-PAE copolymers and OVA were mixed with the final concentration of 5 mg/ml and 1mg/ml.

The entrapment efficiency was measured as total encapsulated OVA weight / initial OVA weight  $\times$  100.

**Figure 1**

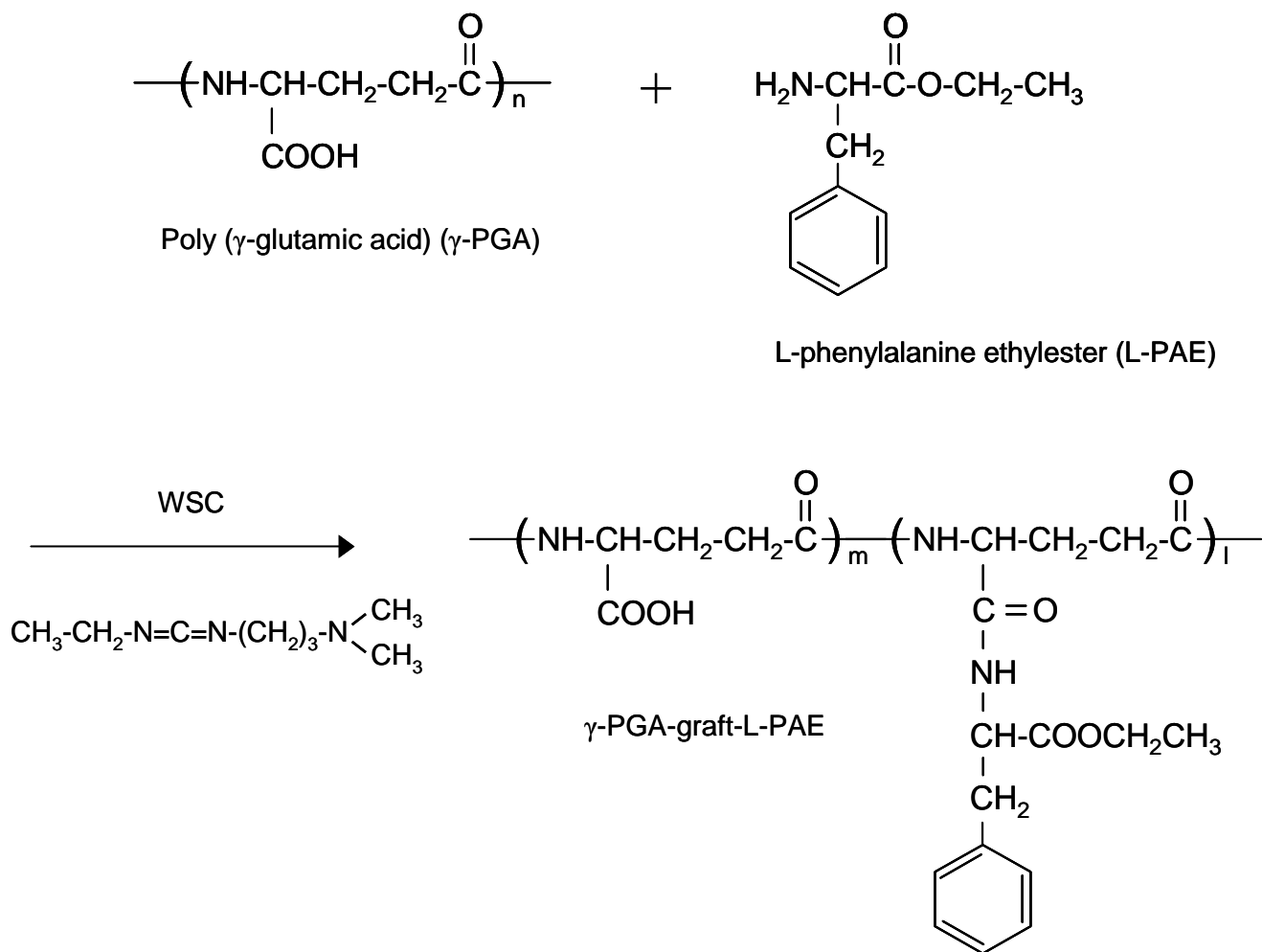
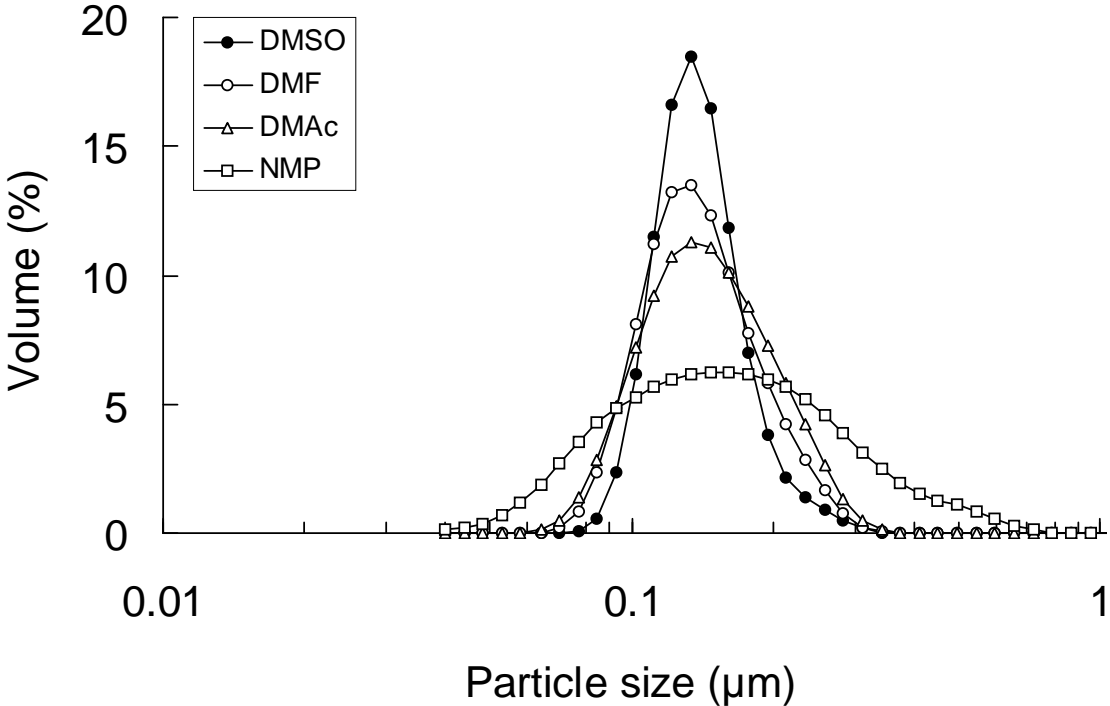


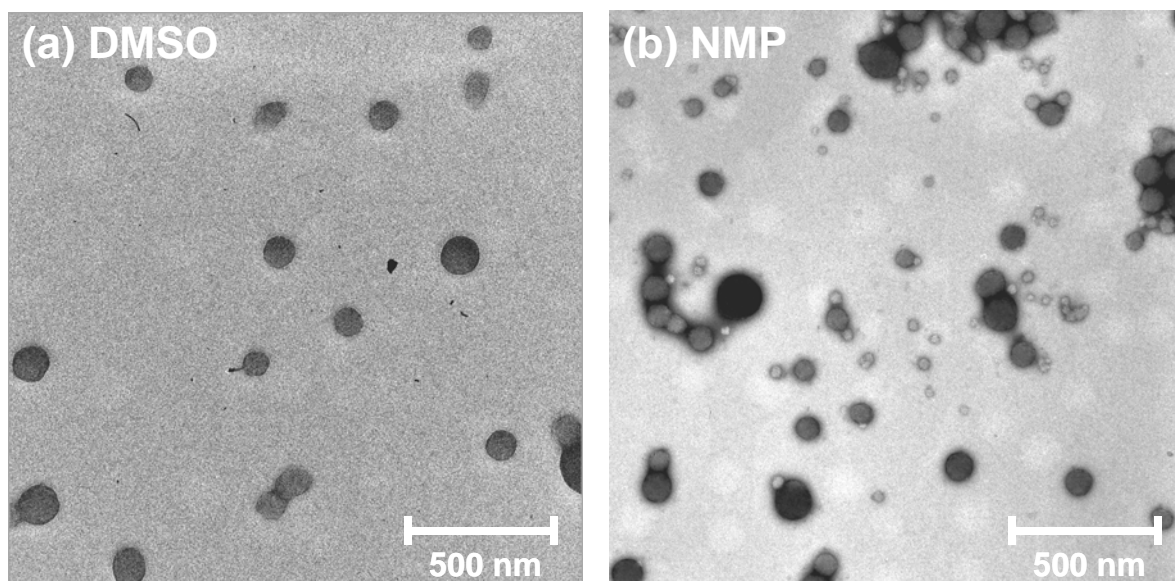
**Figure 2**



**Akagi et al.**

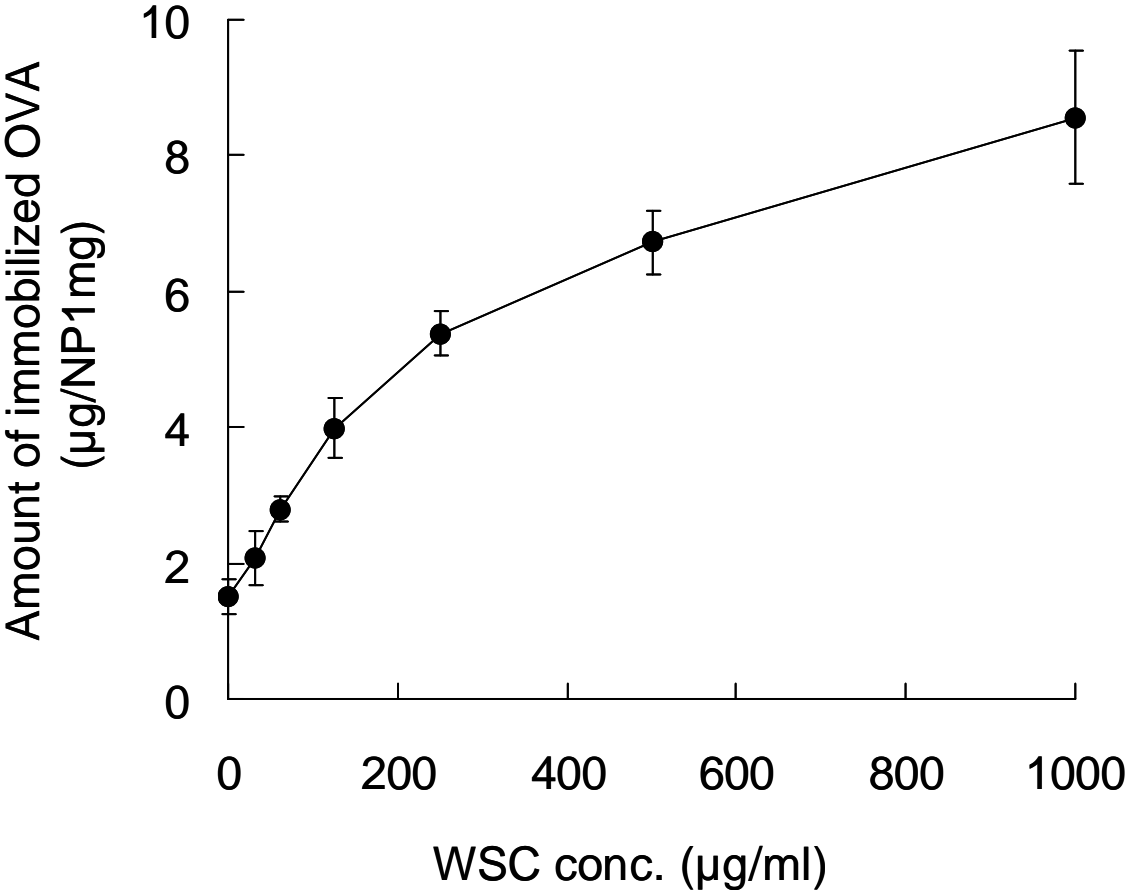


**Figure 3**



**Akagi et al.**

**Figure 4**



**Akagi et al.**

**Figure 5**

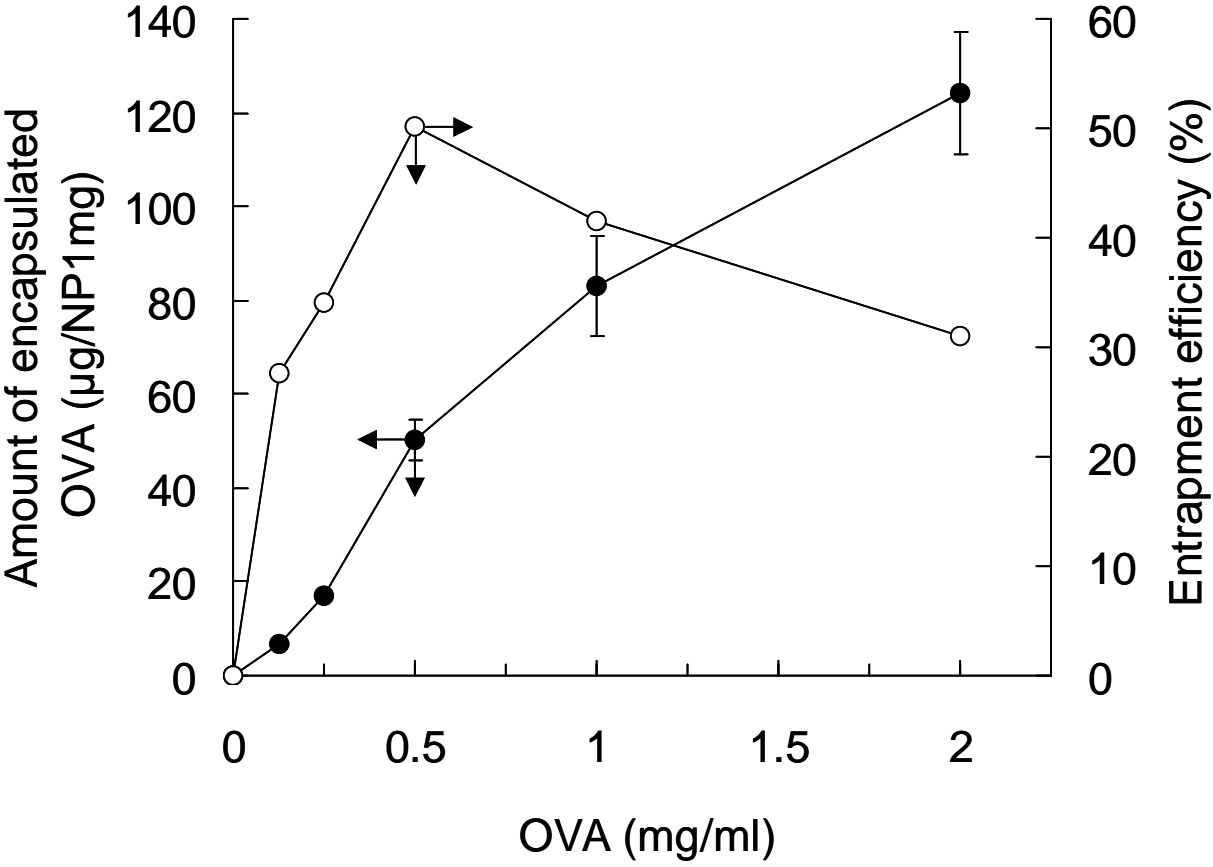
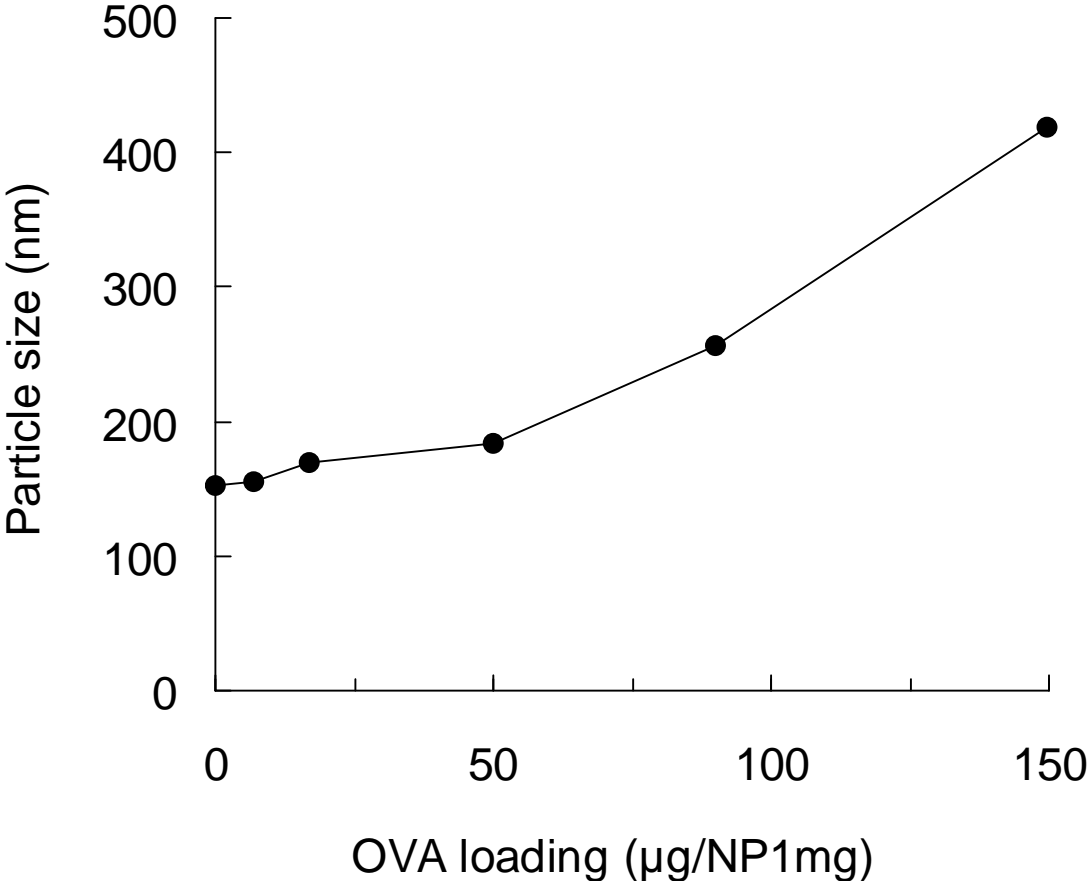
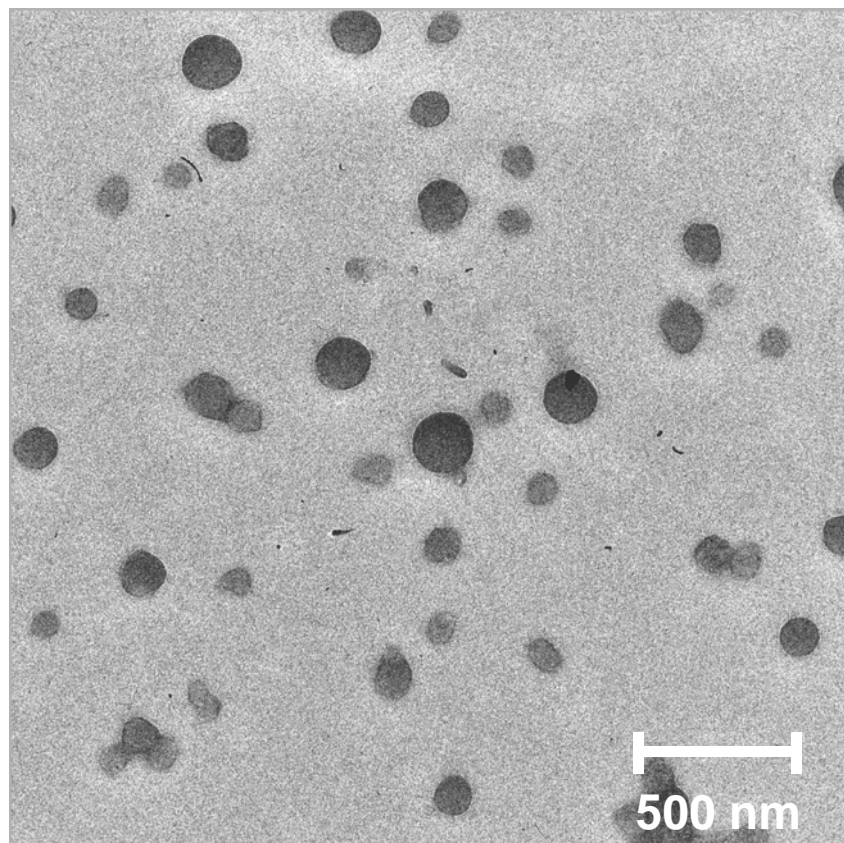


**Figure 6**



**Akagi et al.**

**Figure 7**



**Akagi et al.**

**Figure 8**

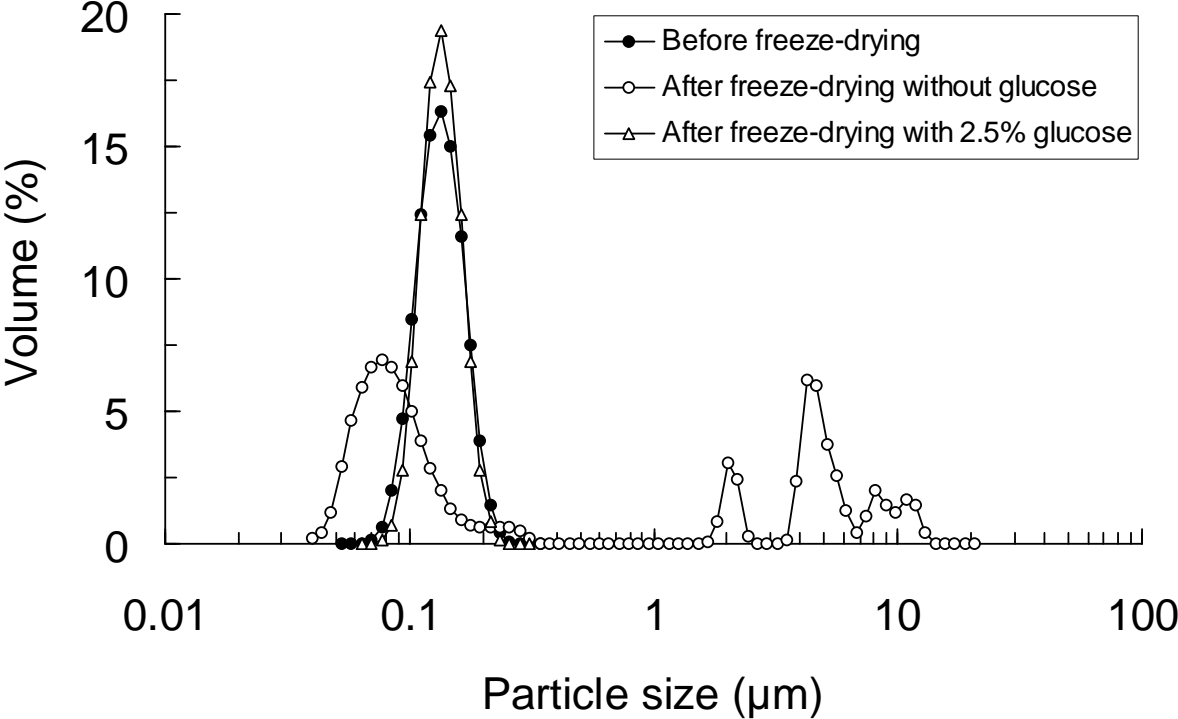
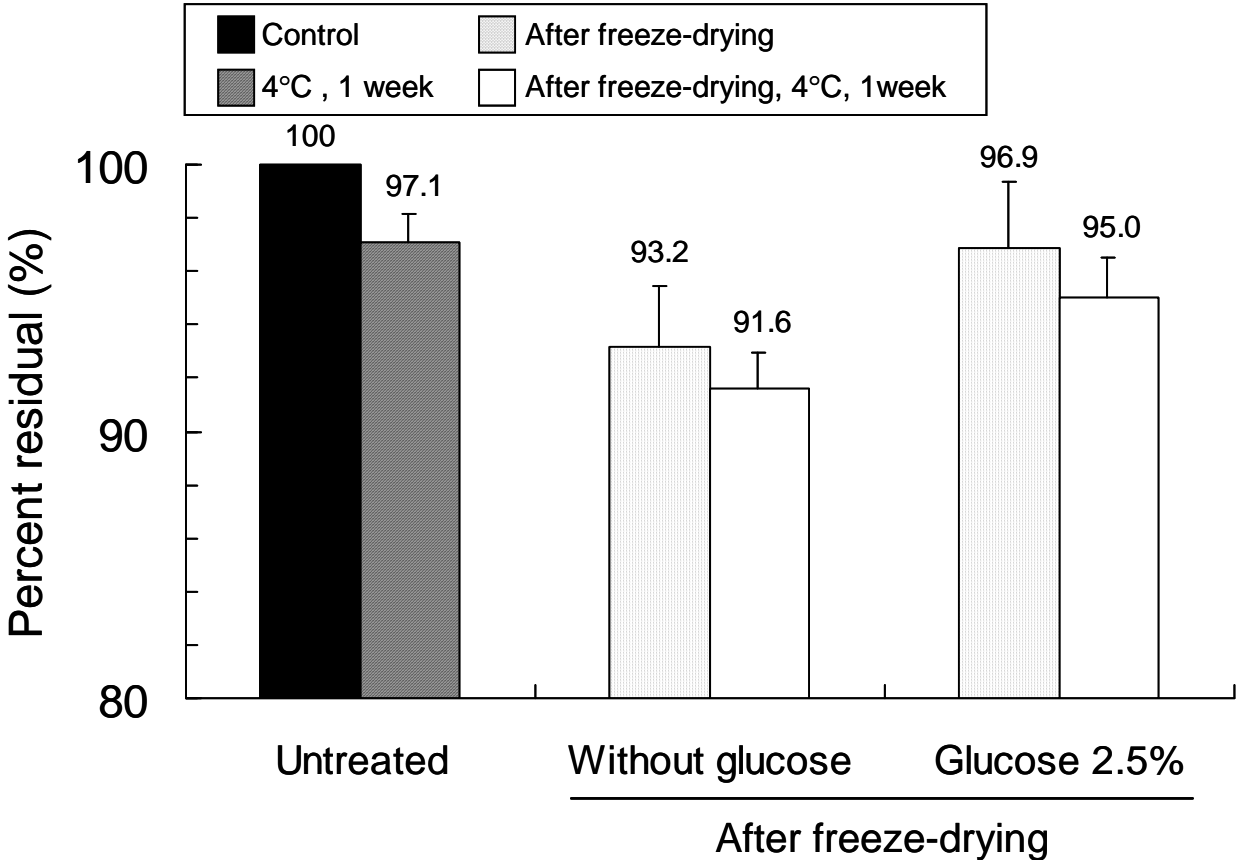
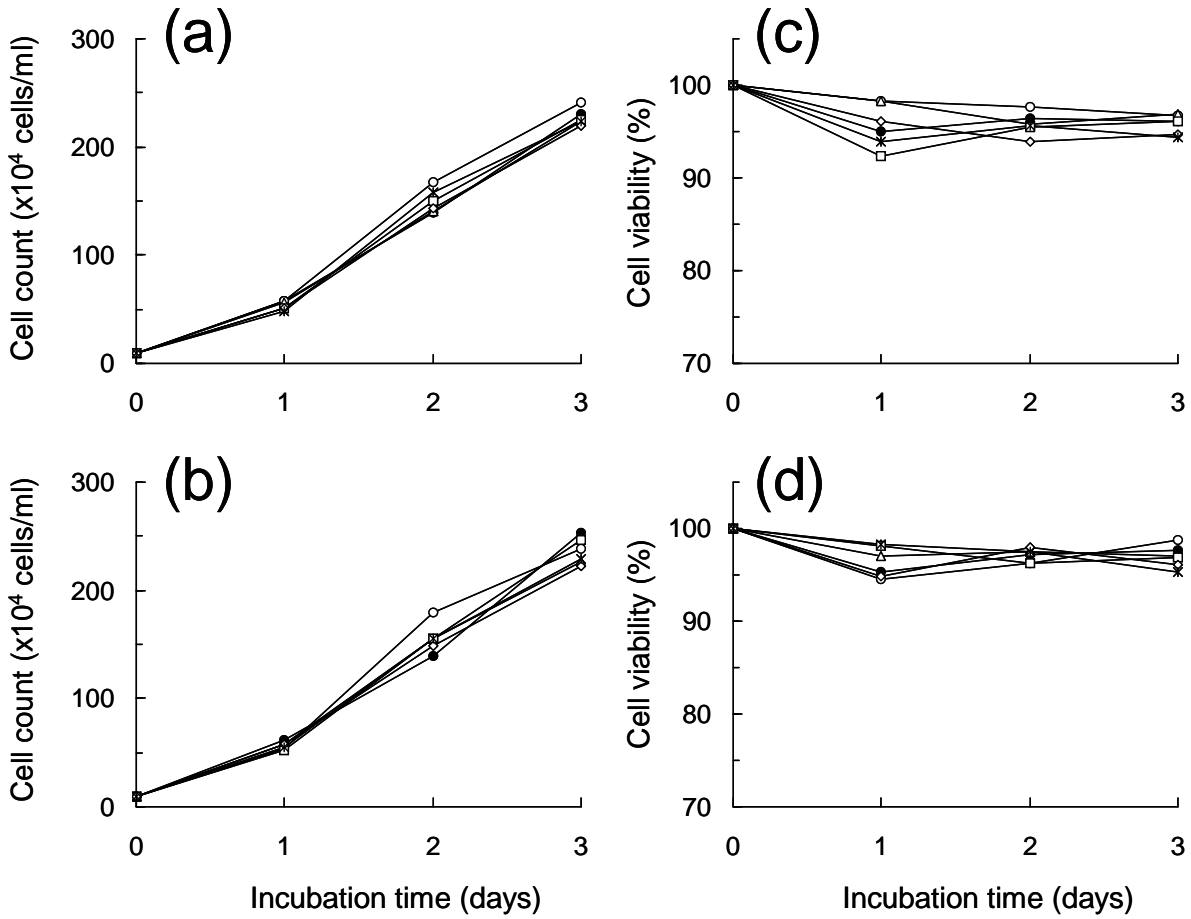


**Figure 9**



**Akagi et al.**

**Figure 10**



**Akagi et al.**